Structure of Phenylalanine-Accepting Transfer Ribonucleic Acid and of Its Environment in Aqueous Solvents with Different Salts†

Zong Qi Li,‡ Richard Giegé, Bernard Jacrot,§ Radulf Oberthür, Jean-Claude Thierry, and Giuseppe Zaccaï*

ABSTRACT: Thermodynamic and structural parameters were measured for brewers' yeast $tRNA^{Phe}$ in solution in the range of 0.1–0.9 M monovalent salt (with and without 1 mM $MgCl_2$), pH 7.0, by small-angle neutron scattering. Partial specific volumes and preferential interaction parameters were found to be similar to corresponding values measured by more conventional means in DNA [Eisenberg, H. (1981) *Q. Rev. Biophys. 14*, 141–172]. There is no evidence of a large conformational change in $tRNA^{Phe}$ in this range, and the molecule has a radius of gyration that is the same as that calculated from the crystal-structure coordinates (23 Å). Transfer RNA in solution is made up of polyion $tRNA^{76-}$ and 76 positive monovalent ions (in absence of Mg^{2+}). The data show the polyion to be surrounded by a shell of solvent that is significantly denser than bulk, whose structure depends on salt conditions. In 0.1 M NaCl, it has an excess mass of ~85 molecules of water. This would be accounted for, for example, by ~850 molecules of water if their density were 10% higher than that for bulk. The radius of gyration of the dense shell is ~30 Å for NatRNA and ~35 Å for KtRNA. The present study shows that the solvent around tRNA is a component of its structure that must be taken into account in understanding its function.

Transfer RNAs are relatively small nucleic acid molecules of about 75 nucleotides each carrying one negative charge at pH 7. When the structure or conformation of a tRNA molecule is evoked, it usually refers to the atoms in the polynucleotide chain [recent review by Ofengand (1982)]. Where biological relevance is concerned, however, this represents only one component of the "structure"; the other is the immediate environment of the molecule: the solvent molecules interacting with it. Because all the functional interactions of the molecule proceed through it, its structure could be as relevant as that of the polynucleotide chain.

The interaction between a solute and solvent can be expressed in terms of measurable thermodynamic variables (Eisenberg, 1981). In general, these variables cannot be used to derive structural molecular parameters because they represent properties of the solution as a whole. There are special cases, however, where an "equivalent particle" occupying a constant volume could be defined, but these do not apply to charged macromolecules (Tardieu et al., 1981).

Small-angle neutron scattering from solution allows a determination of some of these thermodynamic variables in different conditions, simultaneously with particle parameters that would reflect conformational changes (Zaccai & Jacrot, 1983). Neutron scattering measurements on $tRNA^{Phe}$ are presented in this paper. Experiments were designed to obtain structural and thermodynamic parameters for native tRNA and its immediate solvent environment in aqueous solution with different monovalent salts. They have shown that there are no large conformational changes in tRNA beyond 0.1 M monovalent salt and that the solvent environment of the macromolecule depends significantly on salt conditions.

Materials and Methods

Transfer RNA Preparation and Handling. Brewers' yeast $tRNA^{Phe}$ was purified from crude tRNA (Boehringer, Mannheim, Germany) by countercurrent distribution (Dirheimer & Ebel, 1967) followed by conventional chromatographic techniques (Ehrlich et al., 1980). The purified species had a phenylalanine acceptance of 1500 pmol/A_{260} unit. The material was stored as the sodium salt in a dry pellet, which was dissolved in distilled water a few days before the experiment and then dialyzed against 10 mM cacodylate buffer, pH 7.0, with 1 M salt and 5 mM EDTA.[1] Salt was either NaCl or KCl, and water was the appropriate ^2H_2O–H_2O mixture for the experiment. Subsequently, samples were dialyzed against the scattering buffer: 10 mM sodium cacodylate, pH 7.0, the appropriate salt and its concentration (NaCl, KCl), and 0.1 mM EDTA.

Concentration of tRNA was determined by UV absorption. Typically, sample aliquots were diluted by a factor of 500 in either distilled water or buffer containing 10 mM $MgCl_2$. Corresponding absorbance values were 1.59 nmol/A_{260} unit in distilled water and 1.86 nmol/A_{260} unit in magnesium buffer. The uncertainty in these values is about 8% (Guéron & Leroy, 1978). To obtain mass concentration values, molar masses of 26 560 and 27 776 were taken for NatRNA and KtRNA, respectively.

The dialyzed volumes had concentrations of about 12 mg/mL, and experimental concentrations were obtained by dilution in the dialyzing buffer. Different salt concentrations were obtained either by dialysis or direct addition of solution to the measuring cuvette. The two approaches were apparently equivalent above 0.3 M monovalent salt because the initial presence of salt associated with the molecule was negligible. The structural and functional integrity of the sample was verified before and after the experiment by gel electrophoresis (Figure 1) and aminoacylation assays. Polyacrylamide gel

† From the Institut Laue-Langevin, 38042 Grenoble Cédex, France (Z.Q.L., B.J., R.O., and G.Z.), and the Institut de Biologie Moléculaire et Cellulaire du Centre National de la Recherche Scientifique, 67048 Strasbourg Cédex, France (R.G. and J.-C.T.). *Received March 8, 1983.* Part of this work was presented at the Brookhaven Symposium on Neutrons in Biology (June 1982).

‡ Present address: Shanghai Institute of Biochemistry, Academia Sinica, Shanghai, China.

§ Present address: European Molecular Biology Outstation I.L.L., 38042 Grenoble Cédex, France.

[1] Abbreviations: NatRNA, KtRNA, and NaDNA, corresponding salts of transfer RNA and DNA; K nucleotide, nucleotide neutralized by a K^+ ion at pH 7.0; EDTA, (ethylenedinitrilo)tetraacetic acid disodium salt.

0006-2960/83/0422-4380$01.50/0

electrophoresis was performed in the presence of 7 M urea under the solvent system of Maxam & Gilbert (1980); aminoacylation assays were performed as described by Giegé et al. (1972).

Neutron Scattering Experiments. All experiments were performed on D11, the small-angle scattering camera at the Institut Laue-Langevin (Ibel, 1976). Appropriate wavelength and sample-detector distances were chosen to examine an angular range of $0.02 \lesssim Q \lesssim 0.15$ Å^{-1} [$Q = (4\pi \sin \theta)/\lambda$; θ is half the scattering angle; λ is the wavelength]. The wavelength bandwidth was 8%. Samples were placed in quartz spectrophotometer cuvettes of 0.100-cm path for H_2O buffer and 0.200-cm path for ^2H_2O with irradiated volumes of 0.100 and 0.200 cm^3, respectively. All data were collected at room temperature with exposure times of about 0.5 h. Intensity curves were corrected for uniformity of detector response by using the incoherent scattering of water, which also puts the data on an absolute scale (Jacrot & Zaccai, 1981). The background due to the solvent alone was subtracted.

Theory

Forward Scattered Intensity $I(0)$ and Radius of Gyration R_g. When there is no correlation between either the position or the orientation of molecules in solution, their small-angle scattering curve $I(Q)$ could be analyzed in the Guinier approximation (Guinier & Fournet, 1955):

$$I(Q) = I(0) \exp[-(1/3)R_g^2Q^2] \quad (1)$$

where $Q = (4\pi \sin \theta)/\lambda$, 2θ is the scattering angle, and λ is the wavelength. The forward scattered intensity $I(0)$ and R_g^2 are experimental parameters obtained from the intercept and gradient of the ln $I(Q)$ vs. Q^2 straight-line plot. In small-angle scattering, the observed intensity is also affected by interference between the particles (Guinier & Fournet, 1955), and only when there is no correlation between either their positions or their orientations can this be neglected. When the particles are charged, as it is the case for nucleic acids, interference arises from the electrostatic interaction, which is not negligible even at very low concentrations. Because of the possibility of conformational changes with salt concentration, the interparticle interference in the tRNA data could not be removed simply by shielding the charges on the macromolecule in stronger salt solutions. Following Ninio (1970) and Oberthür (1975a), the apparent values of $I(0)$ and R_g^2 obtained from the intensity curves were extrapolated to zero concentration rather than extrapolating the curve itself. Typically, three concentrations were measured for each condition: about ~12, ~6, and ~4 mg/mL. Even so, the electrostatic structure factor did not permit reliable data to be collected below salt concentrations of 0.1 M NaCl or KCl. The extrapolated $I(0)$ and R_g^2 can be related to the structure of the particle or interpreted in terms of thermodynamic variables for the solution.

In the "particle" approach, the expressions for $I(0)$ and R_g are

$$I(0) = (cN_A/M)[\sum_i (b_i - \rho^\circ v_i)]^2 \quad (2)$$

and

$$R_g^2 = \sum_i (b_i - \rho^\circ v_i) r_i^2 / \sum_i (b_i - \rho^\circ v_i) \quad (3)$$

$I(0)$ is from unit volume of sample, c is mass concentration, M is molar mass, and N_A is Avogadro's number; b_i and v_i are the scattering length and volume, respectively, of a group of atoms in the particle, ρ° is the scattering length density of the solvent, r_i is the distance of the group to the center of mass of the $b_i - \rho^\circ v_i$ distribution. The quantity $b_i - \rho^\circ v_i$ is the excess scattering mass or contrast length of the group of atoms. The size of the group must be small compared to the resolution of the experiment (Jacrot, 1976), and the summation in eq 2 and 3 should be performed over the entire volume of the particle, including the solvent, which is perturbed by the macromolecule. The size of this volume is arbitrary provided that outside its boundary, the composition and structure of the solvent are unaffected by the presence of the particle (Zaccai, 1981).

Radius of Gyration Calculation from Crystal Atomic Coordinates. The radius of gyration of $tRNA^{Phe}$ was computed from the atomic coordinates of the crystal structure (Quigley et al., 1975). The contribution of H atoms to the neutron scattering length cannot be neglected, and the coordinates of hydrogen atoms were derived from chemical arguments according to the conformation of each nucleotide. The amino/imino protons of bases and the hydroxyl protons in the ribose were considered to be readily exchangeable with ^2H, i.e., three, four, three, and two protons for adenosine, guanosine, cytidine, and uridine, respectively (Englander et al., 1972; Jacrot, 1976). The minor nucleotides were each treated independently; for example, the C8 proton in m^7G^{46} is known to exchange rapidly (Tomasz, 1970). The radius of gyration in vacuo was calculated from eq 3, ignoring the $\rho^\circ v_i$ terms. In H_2O, these terms are very small so that the radius of gyration in vacuo and in H_2O is expected to be very similar. For the calculation with a general value of ρ°, volumes calculated by A. V. Westerman and J. L. Finney (private communication) were used. These were obtained by dividing up the volume of the molecule into Voronoi polyhedra around each atom and neglecting all interactions with solvent (Finney, 1975).

Thermodynamic Interpretation of Scattering. In the thermodynamic approach of Eisenberg (1981), the interpretation of $I(0)$ is in terms of measurable quantities and does not rely on a particle model. For a three-component system [water (1), macromolecular solute (2), and salt (3)], $I(0)$ is given by

$$I(0) = (c_2M_2/N_A)(\partial\rho/\partial c_2)^2_{\mu \neq \mu_2} \quad (4)$$

and

$$(\partial\rho/\partial c_2)_{\mu \neq \mu_2} = b_2 + \xi_3 b_3 - \rho^\circ(\bar{v}_2 + \xi_3 \bar{v}_3) \quad (5)$$

where subscripts refer to the component, and c is concentration in grams per liter, M is molar mass in grams per mole, μ is chemical potential, ρ is neutron scattering length density of the solution in reciprocal squared centimeters, b is scattering length per gram of component, ξ is an interaction parameter in grams per gram of component 2, ρ° is the scattering length density of the solvent, and $\bar{v}$ is partial specific volume in cubic centimeters per gram.

There are analogous equations for X-ray and light scattering and for equilibrium sedimentation, and Eisenberg has shown how these techniques give overlapping and complementary information (Eisenberg, 1981). Relationships between the particle and thermodynamic interpretations of scattering are discussed by Zaccai & Jacrot (1983).

Contrast Variation by ^2H_2O–H_2O Exchange. Contrast variation in neutron scattering and its limitation have been discussed recently (J. Witz, unpublished results; Zaccai & Jacrot, 1983). The values of b_i and ρ° in eq 2 and 3 are functions of the proportion of ^2H_2O in the solvent—that of b_i because of the exchange of labile hydrogen atoms. Also, in the particle approach, solvent closely associated with the molecule is included in the summations, and its composition

Table I: Parameters from Forward Scattered Intensity–Experimental Values

condition	ρ° (10^9 cm^{-2})	% ^2H_2O equiv	$I'(0)/(cTt)$ (cm^2/g)[a]	$\lvert\partial\rho/\partial c\rvert_{obsd}$ (10^9 cm/g)[b]	match point (% ^2H_2O equiv)	ϕ'_N(obsd) (cm^3/g)[c]
H_2O, 0.1 M NaCl	−5.53	<1	0.42 ± 0.02	21.4 ± 0.5	~74	0.479 ± 0.700
^2H_2O, 0.1 M NaCl	62.6	98	0.047 ± 0.002	7.2 ± 0.2		0.498 ± 0.004
H_2O, 0.9 M NaCl	−4.83	<1	0.43 ± 0.02	21.7 ± 0.5	~71	0.611 ± 0.100
^2H_2O, 0.9 M NaCl	62.4	98	0.0596 ± 0.003	8.1 ± 0.2		0.514 ± 0.003
H_2O, 0.1 M KCl	−5.53	<1	0.40 ± 0.02	20.5 ± 0.5	~69	0.316 ± 0.090
^2H_2O, 0.1 M KCl	62.6	98	0.070 ± 0.003	8.5 ± 0.2		0.504 ± 0.003
H_2O, 0.9 M KCl	−4.78	<1	0.40 ± 0.02	20.5 ± 0.5	~67	0.366 ± 0.100
^2H_2O, 0.9 M KCl	61.9	97	0.084 ± 0.003	9.3 ± 0.2		0.522 ± 0.003

[a] The intensity $I'(0)$ has been normalized by the incoherent scattering of 0.100 cm of H_2O (Jacrot & Zaccai, 1981). c is tRNA concentration (g/L); T is the transmission of the sample (0.52 for H_2O and 0.83 for ^2H_2O); t is the path length in the sample (0.100 cm for H_2O, 0.200 cm for ^2H_2O). [b] $\lvert\partial\rho/\partial c\rvert_{obsd}$ was obtained from $I'(0)/(cTt)$ = constant × $(M/N_A)(\partial\rho/\partial c)^2_{obsd}$ where constant = $10^3 f4\pi/(1 - T_{H_2O})$, see text. [c] Calculated from $\partial\rho/\partial c = b_2 - \rho^\circ\phi'_N$, see text.

depends on the proportion of ^2H_2O as well. All labile hydrogen atoms in tRNA are potentially accessible to solvent and should exchange. In these conditions, the square root of the intensity $I(0)$ is a linear function of the ^2H_2O–H_2O ratio, X, in the solvent. It is assumed that, thermodynamically, the ^2H_2O–H_2O mixture behaves as one component and that interactions with the third component (salt) do not depend on the water isotope ratio. The parameter ξ and partial specific volumes, therefore, are constant with X.

By changing the relative magnitude of the scattering length and volume terms in the expression $b_i - \rho^\circ v_i$, contrast variation allows a separation of their contributions to the scattering. Thus, in H_2O solution, the volume term has very little influence on the data, which is dominated by the polynucleotide chain composition and conformation. In ^2H_2O, on the other hand, the two terms are of similar magnitude, and volume and solvent effects are magnified. Contrast variation allows a separation of the two components of the structure described in the introduction.

A quantitative analysis of radius of gyration dependence on contrast in terms of scattering density fluctuations in the particle has been derived by Ibel & Stuhrmann (1975). The expression for R_g^2 as a function of mean contrast $\bar{\rho}$ (where we define contrast as the difference between the mean scattering density of the particle and that of the solvent) is

$$R_g^2 = R_c^2 + \alpha/\bar{\rho} - \beta/\bar{\rho}^2 \quad (6)$$

where R_c, α, and β are experimental parameters. When there is exchange of labile hydrogen or solvent associated with the particle, their interpretation is not straightforward (Zaccai & Jacrot, 1983; J. Witz, unpublished results). For a particle where the centers of mass of the shape, of fluctuations in density, and in exchange about their mean values coincide, the parameter β is equal to zero, and R_g^2 vs. $1/\bar{\rho}$ is a straight line of slope α. The parameter α is related to the radius of gyration of density and labile H exchange fluctuations about the mean scattering density in the particle. A positive value of α shows the dense parts of the particle to be relatively further from the center of scattering mass and vice versa.

Results

Experimental Data. Typical scattering curves of tRNA are plotted as ln $I(Q^2)$ in Figure 1. The signal to background ratio (i.e., the scattering of the solution compared to the scattering of the solvent) is small and about the same in H_2O and ^2H_2O buffers: in H_2O, the background is larger by a factor of ~5 because of the incoherent scattering of ^1H, and in ^2H_2O, the signal is smaller by a factor of ~5 because of the reduced contrast between tRNA and solvent. Because of this, the data

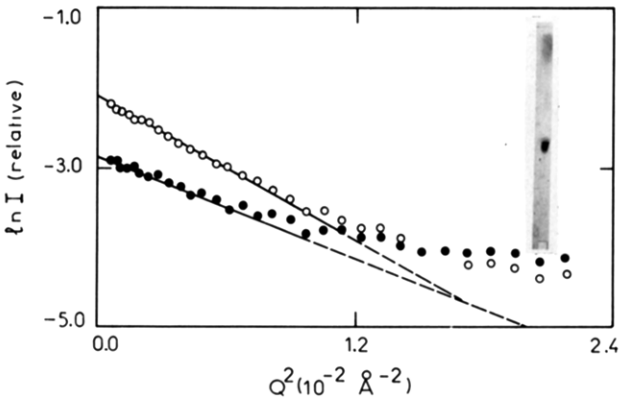

FIGURE 1: Scattering curves of $tRNA^{Phe}$ in the buffer described in the text; salt conditions were 0.1 M NaCl in H_2O (○) and ^2H_2O (●). Concentration of tRNA was 5 g/L in H_2O and 5.5 g/L in ^2H_2O. The intensity is in relative units so that the two curves could be plotted together to show the different slopes. (Inset) Polyacrylamide gel of a $tRNA^{Phe}$ sample performed after the neutron experiments in conditions described under Materials and Methods. The gel was overloaded to show that there are no minor bands, which would have indicated the molecule was degraded.

were quite sensitive to systematic errors such as slight differences between the ^2H content of sample and buffer solutions. Even though the transmission measurement is usually a good check that sample and buffer have the same ^2H content (May et al., 1981), its accuracy was inadequate for the tRNA experiments. Samples were dialyzed extensively in shallow containers to ensure perfect equilibrium with buffers.

Scattering curves were measured as a function of tRNA concentration, and the results [apparent radius of gyration, R_g, and apparent forward scattered intensity normalized by concentration, $I'(0)/c$] are shown in Figure 2 for the 0.1 M NaCl condition. The measured intensity divided by the scattering of 0.100 cm of H_2O in the same experimental conditions is written $I'(Q)$. It is related to the corresponding value $I(Q)$ in absolute units that must be used in eq 1, 2, and 4 by

$$\frac{I'(Q)}{cTt} = [10^3 f4\pi/(1 - T_{H_2O})]I(Q)$$

where T and T_{H_2O} are the transmissions of sample and 0.100 cm of H_2O, respectively, t is sample path length in centimeters, c is mass concentration in grams per liter, and f is a wavelength-dependent parameter close to 1 (Jacrot & Zaccaï, 1981). Salt conditions examined were 0.1–0.9 M NaCl or KCl in the absence of added magnesium salt and the same with 1 mM $MgCl_2$. There was no difference between the results with and without added $MgCl_2$. The experimental values for

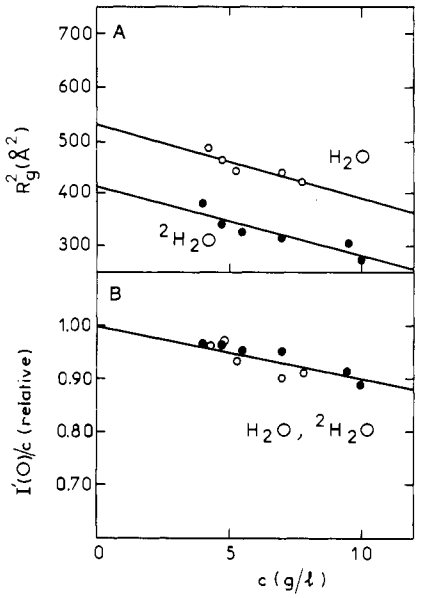

FIGURE 2: Concentration dependence of the Guinier parameters (A) R_g^2 and (B) $I'(0)$, in H_2O (○) and ^2H_2O (●) for 0.1 M NaCl in the buffer. In order to show that the concentration dependence is independent of water isotope, values of $I(0)$ were normalized by their intercept at zero concentration.

the different conditions are shown in Table I. Quoted errors include the statistical uncertainty in the measurements of the scattered intensity, transmission, and concentration but not the uncertainty in the UV absorbance, which introduces the same systematic error for all conditions.

As expected, the apparent Guinier parameters had a smaller concentration dependence in buffers of higher salt concentrations. At and beyond 0.3 M NaCl or KCl, the dependence was negligible in the concentration range examined (data not shown). In what follows, the concentration dependence has been accounted for; R_g and $I'(0)/c$ have been either extrapolated to zero concentration or measured at high salt. The data plotted in Figure 3 have the following qualitative trends: In H_2O, $I'(0)/c$ and R_g are within errors similar in NaCl and KCl and constant for the salt concentration range. In ^2H_2O, $I'(0)/c$ is quite different in NaCl and KCl and, in both cases, increases with salt concentration. Still, in ^2H_2O, R_g does not vary significantly with either the nature of the salt or its concentration, but its value is significantly smaller than the H_2O value. It was verified systematically that the aminoacylation capacity and structural integrity of $tRNA^{Phe}$ remained unaffected by the neutron measurements.

A consequence of the different values of $I'(0)/c$ in ^2H_2O is that the "match point" of tRNA [the ^2H_2O percentage in the buffer for which $I(0)$ vanishes] is a function of solvent conditions. The match points are given in Table I; these were used to calculate $\bar{\rho}$ for the plot of R_g^2 vs. $1/\bar{\rho}$ shown in Figure 4.

Attempts were made to collect data for intermediate ^2H_2O–H_2O ratios in the buffer. But, because of small contrast and high incoherent background, these measurements had very large error bars and did not usefully extend the information from H_2O and ^2H_2O. The R_g^2 dependence on reciprocal mean contrast is shown in Figure 4 with only these two measured points, therefore. Horizontal error bars express the spread in match points for the different salt conditions. If one assumes a straight-line dependence, a positive value of α is found (eq 6).

Thermodynamic Interpretation of Forward Scattered Intensity. By analogy with sedimentation equilibrium [for example, Pundak & Eisenberg (1981)], the scattering density increment in eq 5 is written as

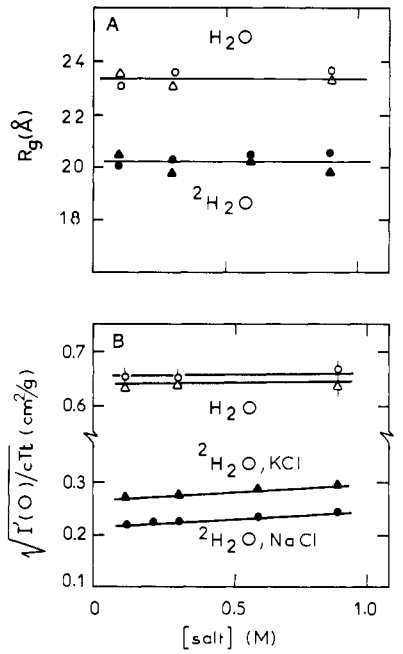

FIGURE 3: Radius of gyration R_g and intensity $[I'(0)/(cTt)]^{1/2}$ as a function of salt for H_2O and ^2H_2O buffers. $I'(0)$ has been normalized by the incoherent scattering of H_2O; c is concentration in grams per liter; T is transmission, and t is path length in centimeters. (●, ○) NaCl in ^2H_2O and H_2O, respectively; (▲, △) KCl in ^2H_2O and H_2O, respectively.

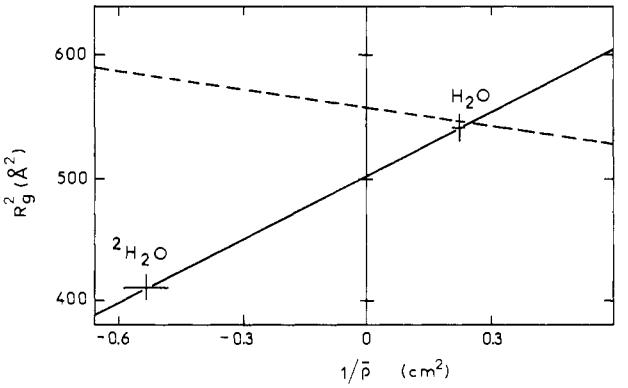

FIGURE 4: Square of radius of gyration as a function of reciprocal mean contrast. The dotted line was calculated from the crystal structure by assuming bulk solvent at the molecular boundary of the tRNA ion (see text).

$$\partial\rho/\partial c = b_2 - \rho^\circ\phi'_N \quad (7)$$

where ϕ'_N has dimensions of partial specific volume. Comparing to eq 5

$$\phi'_N = \bar{v}_2 + \xi_3(\bar{v}_3 - b_3/\rho^\circ)$$

The parameter ϕ'_N contains both the partial specific volume of the macromolecule and an interaction term. To assess their relative magnitudes, values of $\bar{v}_2$ and $\xi_3(\bar{v}_3 - b_3/\rho^\circ)$ have been calculated in H_2O and ^2H_2O with previously published parameters for NaDNA (Cohen & Eisenberg, 1968) and tabulated in Table II, together with b_2 values calculated for tRNA by assuming total exchange of labile H atoms with solvent.

In H_2O, because ρ° is small and negative, $\rho^\circ\phi'_N$ is only about 10% of $\partial\rho/\partial c$. In practice, therefore, data in H_2O are expected to be sensitive to the macromolecule composition alone and not to its partial specific volume or interactions with solvent

Table II: Calculation of Scattering Density Increment $(\partial\rho/\partial c)_{calcd}$ of $tRNA^{Phe}$

condition	ρ° (10^9 cm^{-2})[a]	$\bar{\nu}_2$(DNA) (cm^3/g)[a]	ξ_3(DNA) (g/g)[a]	$\xi_3(\bar{\nu}_3 - b_3/\rho^\circ)$ (DNA) (cm^3/g)[b]	ϕ'_N(DNA) (cm^3/g)	b_2(tRNA) (10^9 cm/g)[c]	$\phi'_N\rho^\circ$ (10^9 cm/g)	$(\partial\rho/\partial c)_{calcd}$ (10^9 cm/g)
0.2 M NaCl, H_2O	−5.44	0.503	−0.04	−0.111	0.392	18.75	−2.13	20.9
0.2 M NaCl, 98% ^2H_2O	62.6	0.503	−0.04	−0.0027	0.500	24	31.3	−7.3
0.976 M NaCl, H_2O	−4.7	0.528	−0.07	−0.222	0.306	18.75	−1.44	20.2
0.976 M NaCl, 98% ^2H_2O	62.4	0.528	−0.07	−0.0046	0.523	24	32.6	−8.6

[a] Values from Cohen & Eisenberg (1968). [b] $\bar{\nu}_3$ for NaCl is 0.284 cm^3/g at 20 °C; $b_3 = 13.6 \times 10^9$ cm/g. [c] b_2 was calculated from the chemical composition of $Na_{76}tRNA$; in ^2H_2O, all labile H are assumed to exchanged with solvent.

components. In ^2H_2O, the situation is quite different: $\rho^\circ\phi'_N$ is a factor of ~4 larger than $\partial\rho/\partial c$ so that changes in ϕ'_N are amplified by the data. The value of ϕ'_N is itself determined by the partial specific volume $\bar{\nu}_2$, the term in ξ_3 representing less than 1% of ϕ'_N. The interaction parameter ξ_3, therefore, cannot be determined from the neutron data because, in H_2O, $\partial\rho/\partial c$ is not sensitive to ϕ'_N and, in ^2H_2O, ϕ'_N is not sensitive to ξ_3.

The basis of our interpretation is that the mass and volume contributions to the solution structure of tRNA are separated by the data in H_2O and ^2H_2O. With an approximate value of ϕ'_N from NaDNA, the intensity data on an absolute scale in H_2O are in very good agreement with the molar mass of NatRNA (Jacrot & Zaccai, 1981). This was used to obtain $|\partial\rho/\partial c|_{obsd}$ and to derive values of ϕ'_N(obsd) for each condition (Table I, eq 4 and 7). Figure 5 is a plot of ϕ'_N(obsd) vs. salt concentrations. A calculation using DNA parameters with b_2 for tRNA (Table II) is also shown in Figure 5a, and there is remarkable agreement between the NatRNA neutron data and the calculated line. The thermodynamic predictions of the neutron data on tRNA, therefore, do not show any special behavior related to its different chemistry and tertiary structure. tRNA appears to behave like DNA in the same salt conditions, and it is likely that this arises from their similar polyelectrolyte natures. In order to derive a more useful parameter than ϕ'_N (which is a function of ρ°), interaction parameters from DNA were used to obtain values of partial specific volume, $\bar{\nu}_2$ (Figure 5b).

Transfer RNA is a different molecule depending on whether it has been dialyzed against NaCl or KCl solvent. In the former, the macromolecule is $Na_{76}tRNA$ (M_r 26 560), and in KCl solvent, it is $K_{76}tRNA$ (M_r 27 776). The molecular weights differ by 5% and so will the concentration in grams per liter at constant nucleotide or phosphate content. The type of salt and method of measuring the concentration are important, therefore, if parameters such as partial specific volume are to be compared in different studies.

Conventional measurements of partial specific volume of tRNA have been reported (Pilz et al., 1977; Nilsson et al., 1982), but because the salt and concentration conditions were insufficiently specified, they cannot be used here. The scattering lengths of Na and K are almost identical so that b_2 also differs by 5%. Values for ϕ'_N(obsd) were derived for the KCl conditions with appropriate values of M and b_2 and are shown in Figure 5a. Note that despite the relatively large difference between $I'(0)$ for KCl and NaCl, the difference in ϕ'_N(obsd) is quite small. The KCl condition was measured for DNA by Strauss et al. (1967), and their interaction parameters were used to calculate $\bar{\nu}_2$ (Figure 5b).

The trends in $\bar{\nu}_2$ are very similar to the one in DNA (Cohen & Eisenberg, 1968). The larger values of $\bar{\nu}_2$ for the KCl

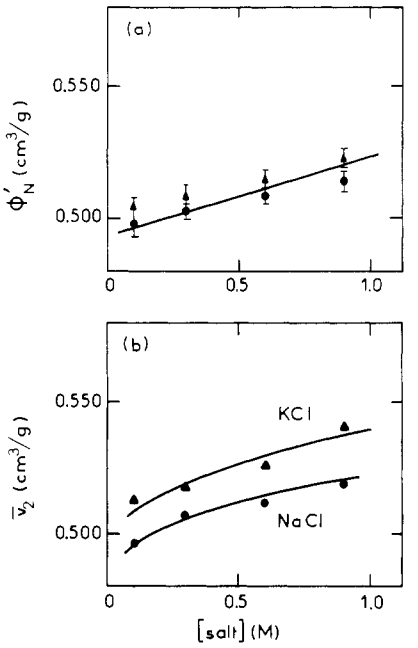

FIGURE 5: (a) Values of volume parameter ϕ'_N(obsd) in ^2H_2O as a function of salt concentration: (●) NaCl; (▲) KCl. The line was calculated by using b_2 for NatRNA and volume parameters from NaDNA (Table II). (b) Values of partial specific volume, $\bar{\nu}_2$, derived from ϕ'_N(obsd) by using interaction parameters from NaDNA.

solutions are readily understood qualitatively in terms of the larger volume per K nucleotide. The thermodynamic interpretation cannot be taken further, and a particle picture is discussed below. In particular, the partial specific volume of a macromolecule is not the volume occupied by the atoms of the macromolecule alone but also includes contributions from density changes in the solvent around it (Zaccai & Jacrot, 1983). Thus, the thermodynamic approach does not allow a separation of these two components, since it measures the volume change of the whole system upon addition of the macromolecules to the solution.

Radius of Gyration and Conformational Changes. By the same arguments presented above for the forward scattered intensity, the radius of gyration in H_2O is essentially sensitive to the spatial arrangement of the atoms in the macromolecule and not to their volume occupation or interactions with solvent (eq 3). Within the limits of experimental accuracy, there is no evidence of a conformational change in the range of conditions examined (Figure 3A). It encompasses the change between 0.1 and 0.2 M NaCl in the presence of 1 mM $MgCl_2$ where Olson et al. (1976) have observed a 12% decrease in the diffusion coefficient. This change, therefore, could not be due to an increase of 12% in radius of gyration of the poly-

nucleotide chain in these conditions.

The neutron scattering length radius of gyration of yeast $tRNA^{Phe}$ in vacuo was calculated from the crystal structure coordinates as explained above. A value of 23.3 Å was found in excellent agreement with the measurements in H_2O. Subtle differences between crystal and solution conformation cannot be excluded of course, but it is clear that the crystal structure is a very good model for the solution conformation in the range of conditions examined.

Dense Solvent around tRNA. From the crystal structure coordinates, a radius of gyration can be calculated in any contrast with eq 3, provided the exchange of labile H is known, the volumes occupied by the atoms are known, and the limits of the summation are taken to include solvent whose characteristics are different from those of bulk solvent. To assess the importance of the perturbed solvent contribution, R_g^2 was calculated as a function of contrast from the crystal structure, assuming no solvent perturbation; i.e., bulk solvent starts right at the macromolecular boundary. The calculated line is shown in Figure 4. It crosses the data line close to the H_2O point as expected; otherwise, it has a negative α (because of the labile H in the base pairs close to the macromolecule core) in complete qualitative disagreement with the measured values in ^2H_2O. If one excludes a conformational change of the macromolecule between H_2O and ^2H_2O (small-angle X-ray measurements of $tRNA^{Phe}$ in both solvents give the same R_g; Z. Q. Li and C. Berthet-Colominas, unpublished results), the solvent perturbation appears to be predominant in determining the ^2H_2O radii of gyration. The positive value of α requires this perturbation to be an increase in solvent density around the macromolecule.

Discussion

Before the publication of the crystal structure of $tRNA^{Phe}$ by Kim et al. (1974) and Robertus et al. (1974), considerable effort was directed toward finding the structure of the molecule by various solution methods [for example, the X-ray small-angle studies of Pilz et al. (1971) and Ninio et al. (1972)]. Since, and especially following the crystal structures of a number of tRNAs, all showing a characteristic L shape (Shevitz et al., 1979; Woo et al., 1980; Moras et al., 1980), the question has shifted to the relationship between solution and crystal structures and to conformational changes in different conditions [review by Schimmel & Redfield (1980) and Favre & Thomas (1981)].

Cole et al. (1972) have established the phase diagram of tRNA as a function of temperature and sodium ion concentration. They show that at normal temperatures and low salt the molecule is extended, presumably because of repulsion between its charged groups, and about 0.1 M NaCl is required for its native conformation. There is extensive evidence, however, in favor of native tRNA having different conformations in solution, depending on solvent conditions.

The functional behavior of tRNA has been explored in different solvents by Yarus (1972), who invoked conformational changes to account for his observations. In particular, a "looser" conformation is suggested for the molecule in special solvent conditions. Physical studies have suggested that these conformational changes could be large. Olson et al. (1976), for example, found the diffusion coefficient of tRNA to decrease by 12% in going from 0.1 to 0.2 M NaCl in the presence of 1 mM $MgCl_2$ and suggested a conformational transition to a less compact structure in the higher salt concentration [see also Potts et al. (1981)]. Following a different experimental approach, Ehrenberg et al. (1979) proposed an equilibrium of three states for $tRNA^{Phe}$ in solution, depending on

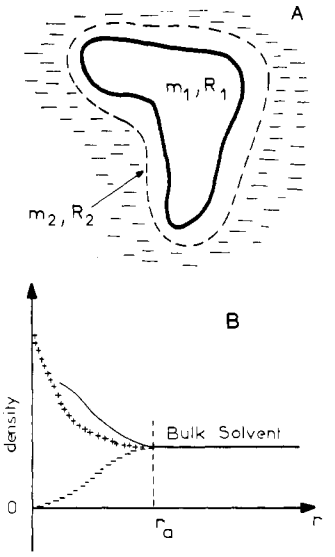

FIGURE 6: (A) Model for tRNA, see text. (B) Schematic diagram of the distributions of water density (—), counterion (+), and co-ion (– –) density around tRNA, as a function of r, the distance from the surface, according to Debye–Hückel theory.

magnesium concentration and temperature, characterized by different relaxation times of fluorescence probes attached to the molecule. Ehrlich et al. (1980) studied the local conformation of the anticodon loop in $tRNA^{Phe}$ by observing the intrinsic fluorescence of the wybutine base. They showed that the molecule is in at least two states in a magnesium-dependent equilibrium. Conformational changes in tRNA–tRNA complexes have also been suggested (Nilsson et al., 1982).

In the present work, $tRNA^{Phe}$ was studied in the range of 0.1–0.9M monovalent salt (with or without 1 mM $MgCl_2$). Its conformation was found to be similar to the crystal structure with no evidence of a large conformational change such as the one reported by Olson et al. (1976). In a more recent study of the translational diffusion of $tRNA^{Phe}$, however, it is suggested that the differences observed with salt concentration are primarily due to alteration in the hydration around the molecule (Fritzinger & Fournier, 1982), in agreement with our observations.

The neutron data are completely consistent with independently determined thermodynamic variables, which are functions of salt conditions (Figure 5). They also show the tRNA molecule to be surrounded by a denser than bulk volume of solvent (Figure 4). The crystal model is adopted for tRNA in order to interpret the ^2H_2O data in terms of exchange of labile H and volume effects such as perturbations in the density of the solvent around the macromolecule.

Because of the polyelectrolyte nature of tRNA, it is expected that some of the water molecules surrounding it should be denser than bulk. Theory predicts an accumulation of positive counterions close to the macromolecule (Guéron & Weisbuch, 1980), and their electrostriction of water is well-known (Millero, 1972). Also, the sum of the volumes calculated from the crystal structure is greater than the molecular volume predicted from the partial specific volume, showing that there is a volume-*decrease* contribution from the solvent. This is in contrast to volume calculations on protein crystal structures [e.g., Finney (1975)] where the total volume is accounted for by the partial specific volume. The neutron data provide an opportunity to quantify the amount of perturbed water and its distribution as a function of salt.

The model proposed is shown in Figure 6. The inner component is the macromolecule in the crystal-structure

Table III: Values Derived for Model Parameters from ^2H_2O Data (See Text and Figure 6)

condition	m_1 (10^{-12} cm)[a]	m_2 (10^{-12} cm)[a]	excess mass (no. of water molecules)	C^+ (10^{-12} cm)[b]
0.1 M NaCl	−472	161 ± 10	85	80
0.9 M NaCl	−472	146 ± 10	77	80
0.1 M KCl	−472	100 ± 10	53	0
0.9 M KCl	−472	42 ± 10	22	0

[a] Calculated from a match point of 65% ^2H_2O for m_1 and the observed match point for $m_1 + m_2$. [b] C^+ is the excess scattering length calculated for 76 counterions by using their infinite-dilution partial specific volumes (−6 cm³/mol for Na^+, 3 cm³/mol for K^+).

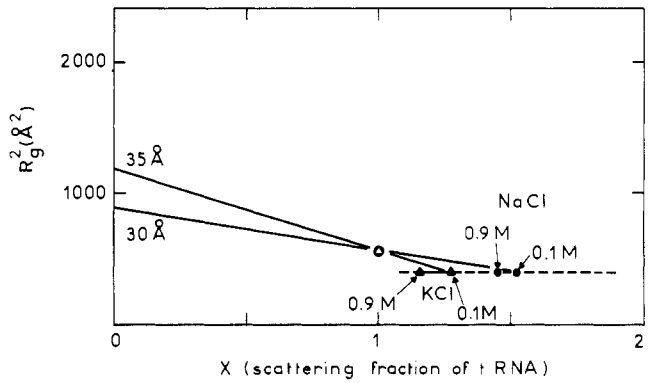

FIGURE 7: R_g^2 vs. x, the scattering fraction $m_1/(m_1 + m_2)$, for the different salt conditions in ^2H_2O. The crystal radius of gyration is plotted at $x = 1$. The value of x for the different salt conditions indicated depends on the match point assumed for component 1 (see text). The dashed line shows where the points would shift if a different match point were taken.

conformation. From the calculated molecular volume, its match point is 65% ^2H_2O. Its excess scattering length, m_1, can be calculated at any contrast from this value and its chemical composition. Its radius of gyration, R_1, is from the dotted line in Figure 4. The outer component is the perturbed solvent with corresponding parameters m_2 and R_2, which shall be derived from the data. It is assumed that the centers of mass of the two components coincide. Then, from the parallel axes theorem for radii of gyration

$$R_g^2 = R_1^2 x + (1 - x)R_2^2$$

where $x = m_1/(m_1 + m_2)$, R_g is the measured radius of gyration for a given condition (salt and contrast), $m_1 + m_2$ is calculated from the observed match point for this condition, and m_1 and R_1 are calculated from the crystal structure. The values derived from m_1 and m_2 in ^2H_2O are in Table III, and a plot of R_g^2 vs. x is shown in Figure 7. To account for the exchanged H in the molecule, R_1 is the value calculated in ^2H_2O. The values of R_2 found are 30 ± 1 Å for 0.1 M NaCl and 35 ± 1 Å for 0.1 M KCl. These values could be systematically higher or lower if the match point were different than 65% ^2H_2O for the tRNA molecule alone. This would change both m_1 and m_2, moving the points in Figure 7 along the dashed line. The value of m_2 is the excess scattering length in the solvent shell around the tRNA ion. As such, it is directly related to the *excess mass* of solvent in this shell (i.e., the mass in the shell minus the mass of an equal volume of bulk solvent). This excess mass corresponds to 85 molecules of water in 0.1 M NaCl, to 77 molecules in 0.9 M NaCl, to 53 molecules in 0.1 M KCl, and to 22 molecules in 0.9 M KCl (see Table III). It is progressively smaller, therefore, in higher salt concentrations and in going from Na^+ to K^+ counterions. This excess mass value has a simple meaning. For example, in 0.1 M NaCl, if there were 850 molecules; the density increase would be smaller than 10% if it affected more than 850 molecules.

The model can be interpreted by Debye–Hückel theory. According to a simple application of this theory (Guéron & Weisbuch, 1980; Oberthür, 1975b), the polyion is surrounded by a water shell containing only positive counterions. Their concentration in the shell is not constant but decays from a large concentration close to the polyion to the concentration of the bulk salt containing solvent over a distance r_a which is a function of the salt concentration in the solvent (Figure 6B). The number of counterions in this shell is of the order of the 76 belonging to the tRNA molecule, so that the molecule can be imagined as shedding part of itself into the water immediately around it. In so doing, it repulses the salt molecules from that volume of water. This gives rise to the negative interaction parameter for salt, ξ_3. An important point to appreciate is that this water shell does not contain salt (for example, NaCl) but does contain a relatively high concentration of positive counterions (for example Na^+); these counterions, however, should be considered to be part of the macromolecule (Na_{76}tRNA) and not part of the salt. The neutron data presented in this paper provide experimental values for the mean density and location of this water shell around the tRNA polyion. Because of electrostriction, it is not surprising to find that the water in the shell is of higher density than bulk. Also, the electrostriction for K^+ is smaller than for Na^+ so that, qualitatively, the smaller values of excess mass found with K^+ can be accounted for. It is more difficult to understand the behavior as a function of salt concentration. In thermodynamic experiments on DNA, $\bar{v}_2$ was observed to increase with salt concentration (Cohen & Eisenberg, 1968). The neutron results on tRNA show the same effect; it corresponds to a decreasing excess mass of water in the shell, with increasing salt concentration. Now, Debye–Hückel theory predicts a smaller volume for the water shell at higher salt concentrations, but the number of counterions in it is not affected much (Guéron & Weisbuch, 1980). The implication is that the electrostriction caused by the counterions is not a constant but depends on local conditions.

The mean partial volume of the 76 counterions in the water shell around tRNA can be derived from the experimental excess water mass values. For Na^+, $\bar{v} \sim -17$ cm³/mol is found in 0.1 M NaCl, decreasing to ~ -14 cm³/mol in 0.9 M NaCl. For K^+, the corresponding values are ~ -9 cm³/mol and ~ -4 cm³/mol. These can be compared to the infinite dilution values for Na^+, $\bar{v} = -6$ cm³/mol, and K^+, $\bar{v} = 3$ cm³/mol (Millero, 1972). Even though the experimental errors are relatively large, the observed values clearly show that there is more electrostriction around tRNA than expected from the infinite dilution partial specific volume of the positive counterions that are used to calculate C^+ in Table III. When it is considered, however, that the local conditions in the water shell are those of a relatively high concentration of only positive ions adjacent to a surface of regularly spaced negative charges, there is no reason to expect the infinite dilution partial volumes to be applicable.

The interaction parameter for DNA at 0.1 M salt (Cohen & Eisenberg, 1968) would correspond to about 5000 molecules of water per molecule of tRNA. Clearly, the perturbation could be spread continuously over a large number of water molecules with a small mean density charge. Both m_2 and R_2 (Figure 6A), however, are not sensitive to the details of how the perturbation is distributed. The relatively large values of R_2 show quite clearly that the perturbed solvent lies further from the center of mass than the tRNA molecular boundary (for example, it is not restricted to the double-helix grooves). Also, the difference in R_2 between NatRNA and KtRNA suggests that the Na^+ ions lie, on average, closer to the macromolecule than do the K^+ ions.

Conclusions

Although the experiments in this study have been performed on $tRNA^{Phe}$, the results should be applicable to transfer RNA molecules in general. Transfer RNA in solution can be considered as having two components to its structure. The first is the conformation of the polynucleotide chain, which has, so far, been implicated in most structure–function discussions. The second has been neglected somewhat even though it was known to exist from the polyelectrolyte nature of the macromolecule; it is the solvent shell around it, which has a different structure from bulk solvent. The present paper has shown that the extent and location of this shell depends on the solvent environment. The biological function of tRNA is strongly affected by its environment. Two independent studies have recently shown how its ability to be aminoacylated and form specific complexes with proteins was not affected in very high concentrations of $(NH_4)_2SO_4$ (1.6 M), whereas in less than 1 M NaCl these were abolished (Giegé et al., 1982; Antonsson & Leberman, 1982). It is not clear why $(NH_4)_2SO_4$ behaves in this way. By analogy with a discussion of the effect of glycerol on proteins, however, a good working hypothesis would be to assume that it affects the solvent environment or "hydration" of the macromolecules rather than their conformation (Gekko & Timasheff, 1981; Lehmann & Zaccai, unpublished results).

Acknowledgments

We are grateful to C. Berthet-Colominas (EMBL, Grenoble) for performing X-ray control experiments on tRNA, to A. V. Westerman and J. L. Finney (Birkbeck College, London) for communication of volume occupation calculations on the tRNA crystral structure, and to P. Morin (Montpellier) for contribution in the early part of this work. We also thank M. Guéron (Ecole Polytechnique, Palaiseau) and D. Moras (IBMC, Strasbourg) for illuminating scientific discussions.

Registry No. NaCl, 7647-14-5; KCl, 7447-40-7.

References

Antonsson, B., & Leberman, R. (1982) *Biochimie 64*, 1035–1040.

Cohen, G., & Eisenberg, H. (1968) *Biopolymers 6*, 1077–1100.

Cole, P. A., Yang, S. K., & Crothers, D. M. (1972) *Biochemistry 11*, 4358–4368.

Dirheimer, G., & Ebel, J. P. (1967) *Bull. Soc. Chim. Biol. 49*, 1679–1687.

Ehrenberg, M., Rigler, R., & Wintermeyer, W. (1979) *Biochemistry 18*, 4588–4599.

Ehrlich, R., Lefèvre, J. L., & Remy, P. (1980) *Eur. J. Biochem. 103*, 145–153.

Eisenberg, H. (1981) *Q. Rev. Biophys. 14*, 141–172.

Englander, J. J., Kallenbach, N. R., & Englander, S. W. (1972) *J. Mol. Biol. 63*, 153–169.

Favre, A., & Thomas, G. (1981) *Annu. Rev. Biophys. Bioeng. 10*, 175–195.

Finney, J. L. (1975) *J. Mol. Biol. 96*, 721–732.

Fritzinger, D. C., & Fournier, M. J. (1982) *Biochemistry 21*, 2118–2127.

Gekko, K., & Timasheff, S. N. (1981) *Biochemistry 20*, 4677–4686.

Giegé, R., Kern, D., & Ebel, J. P. (1972) *Biochimie 54*, 1245–1255.

Giegé, R., Lorber, B., Ebel, J. P., Moras, D., Thierry, J. C., Jacrot, B., & Zaccai, G. (1982) *Biochimie 64*, 357–362.

Guéron, M., & Leroy, J. L. (1978) *Anal. Biochem. 91*, 691–695.

Guéron, M., & Weisbuch, G. (1980) *Biopolymers 19*, 353–382.

Guinier, A., & Fournet, G. (1955) *Small Angle Scattering of X-rays*, Wiley, New York.

Ibel, K. (1976) *J. Appl. Crystallogr. 9*, 630–643.

Ibel, K., & Stuhrmann, H. B. (1975) *J. Mol. Biol. 93*, 255–265.

Jacrot, B. (1976) *Rep. Prog. Phys. 39*, 911–953.

Jacrot, B., & Zaccai, G. (1981) *Biopolymers 20*, 2413–2426.

Kim, S. H., Suddath, F. L., Quigley, G. J., McPherson, A., Sussman, J. C., Wang, A. H. J., Seeman, N. C., & Rich, A. (1974) *Science (Washington, D.C.) 185*, 435–440.

Maxam, A. M., & Gilbert, W. (1980) *Methods Enzymol. 65*, 497–559.

May, R. P., Haas, J., & Ibel, K. (1981) *J. Appl. Crystallogr. 15*, 15–19.

Millero, F. J. (1972) in *Water and Aqueous Solutions* (Horne, R. A., Ed.) Wiley-Interscience, New York.

Moras, D., Comarmond, M. B., Fischer, J., Weiss, R., Thierry, J.-C., Ebel, J. P., & Giegé, R. (1980) *Nature (London) 288*, 669–674.

Nilsson, L., Rigler, R., & Laggner, P. (1982) *Proc. Natl. Acad. Sci. U.S.A. 79*, 5891–5895.

Ninio, J. (1970) Thèse Doctorat d'Etat, Université de Paris.

Ninio, J., Luzzatti, V., & Yaniv, M. (1972) *J. Mol. Biol. 71*, 217–229.

Oberthür, R. C. (1975a) *Makromol. Chem. 176*, 3593–3603.

Oberthür, R. C. (1975b) Dissertation, Mainz.

Ofengand, J. (1982) in *Protein Biosynthesis in Eukaryotes* (Perez-Bercoff, R., Ed.) pp 1–67, Plenum Press, New York.

Olson, T., Fournier, M. J., Langley, K. H., & Ford, N. C. (1976) *J. Mol. Biol. 107*, 193–203.

Pilz, I., Kratky, O., Von der Haar, F., & Cramer, F. (1971) *Eur. J. Biochem. 18*, 436–441.

Pilz, I., Malnig, F. Kratky, O., & Von der Haar, F. (1977) *Eur. J. Biochem. 75*, 35–41.

Potts, R. O., Ford, N. C., & Fournier, M. J. (1981) *Biochemistry 20*, 1653–1659.

Pundak, S., & Eisenberg, H. (1981) *Eur. J. Biochem. 118*, 463–470.

Quigley, G. J., Seeman, N. C., Wang, A. H., Suddath, F. L., & Rich, A. (1975) *Nucleic Acids Res. 2*, 2329–2341.

Robertus, J. D., Ladner, J. E., Finch, J. T., Rhodes, D., Brown, R. S., Clark, B. F. C., & Klug, A. (1974) *Nature (London) 150*, 546–551.

Schimmel, P. R., & Redfield, A. G. (1980) *Annu. Rev. Biophys. Bioeng. 9*, 181–221.

Shevitz, R. W., Podjarny, A. D., Krishnamari, N., Hughes, J. J., Sigler, P. B., & Sussman, J. L. (1979) *Nature (London) 278*, 188–190.

Strauss, U. P., Halfgott, C., & Pinck, H. (1967) *J. Phys. Chem. 71*, 2550–2556.
Tardieu, A., Vachette, P., Gulik, A., & le Maire, M. (1981) *Biochemistry 20*, 4399–4406.
Tomasz, M. (1970) *Biochim. Biophys. Acta 199*, 18–28.
Woo, N. H., Roe, B. A., & Rich, A. (1980) *Nature (London) 286*, 346–351.
Yarus, M. (1972) *Biochemistry 11*, 2050–2060.
Zaccai, G. (1981) in *Scattering Techniques Applied to Supramolecular and Nonequilibrium Systems* (Chen, S. H., Chu, B., & Nossal, R., Eds.) pp 615–638, Plenum Press, New York.
Zaccai, G., & Jacrot, B. (1983) *Annu. Rev. Biophys. Bioeng. 12*, 139–157.

Ubiquitin Adenylate: Structure and Role in Ubiquitin Activation†

Arthur L. Haas,‡ Jessie V. B. Warms, and Irwin A. Rose*

ABSTRACT: The acid precipitate of the ubiquitin activating enzyme after reaction with ATP and ubiquitin contains one enzyme equivalent of ubiquitin adenylate in which the carboxyl-terminal glycine of ubiquitin and AMP are in an acyl–phosphate linkage. The recovered ubiquitin adenylate has the catalytic properties proposed for it as a reaction intermediate. Thus, upon reaction with fresh enzyme in the absence of Mg^{2+} or ATP, the product complex, E–ubiquitin·AMP–ubiquitin, is formed. This complex is capable of generating ubiquitin–protein isopeptide derivatives when added to a reticulocyte fraction that catalyzes protein conjugation. This reproduces the effect previously shown to require ubiquitin, ATP, and Mg^{2+}. In the presence of activating enzyme, ubiquitin adenylate is converted to ATP and free ubiquitin in a step requiring PP_i and Mg^{2+}. On the basis of studies of [^{32}P]PP_i/nucleoside triphosphate exchange, the activating enzyme could be used to generate 2′-deoxy-AMP–, 2′-deoxy-IMP–, and 2′-deoxy-GMP–ubiquitin but not pyrimidine nucleotide–ubiquitin derivatives. The enzyme shows a modest preference for the *pro-S* diastereomers of adenosine 5′-*O*-(1-thiotriphosphate) and adenosine 5′-*O*-(2-thiotriphosphate). Inorganic phosphate, arsenate, methyl phosphate, and tripolyphosphate, but not nucleoside triphosphates, can serve as alternate substrates in place of PP_i in the reverse of ubiquitin adenylate formation. Therefore, the enzyme catalyzes the unusual reaction ATP + P_i ⇌ ADP + PP_i in the presence of ubiquitin.

A novel mechanism of protein modification has recently been described in which a low molecular weight polypeptide (M_r 8556), ubiquitin, is covalently conjugated to target proteins (Ciechanover et al., 1980; Hershko et al., 1980; Wilkinson et al., 1980). In the soluble fraction of reticulocytes (Ciechanover et al., 1980; Hershko et al., 1980, 1982) and other cells (Chin et al., 1982; Hershko et al., 1982), ubiquitin conjugation probably serves as the committed step of energy-dependent protein degradation (Haas & Rose, 1981). In the nucleus, ubiquitin conjugation to core histones 2A (Goldknopf & Busch, 1977) and 2B (Wu et al., 1981) may participate in regulating chromatin structure and subsequent transcription (Levinger & Varshavsky, 1982), as has been recently reviewed by Busch & Goldknopf (1981).

The enzyme responsible for the activation of ubiquitin for the subsequent formation of covalent conjugates with lysine ϵ-amino residues of target proteins is a dimer of 105-kilodalton subunits (Ciechanover et al., 1982; Haas et al., 1982). The steps catalyzed by the ubiquitin activating enzyme are known in some detail but may be condensed to three steps:

$$E_{SH} + ATP + Ub \rightleftharpoons E_{SH}^{AMP\text{-}Ub} + PP_i \quad (1)$$

$$E_{SH}^{AMP\text{-}Ub} \rightleftharpoons E_{S\text{-}Ub} + AMP \quad (2)$$

$$E_{S\text{-}Ub} + ATP + Ub \rightleftharpoons E_{S\text{-}Ub}^{AMP\text{-}Ub} + PP_i \quad (3)$$

The initial formation of a tightly bound ubiquitin adenylate (AMP–Ub)[1] in step 1 is followed by ubiquitin transfer to a thiol group of the same enzyme to form a covalent enzyme–ubiquitin thiol ester, with liberation of AMP (step 2). Activation of a second molecule of ubiquitin yields a stable ternary complex composed of 1 equiv each of ubiquitin adenylate and ubiquitin thiol ester per enzyme subunit (step 3). Stoichiometric evidence and kinetic evidence for this minimal mechanism have been presented previously (Haas et al., 1982; Haas & Rose, 1982). Ubiquitin-dependent ATP/PP_i and ATP/AMP equilibrium isotope exchange kinetics demonstrate that binding of substrates and release of products are strictly ordered, with ATP the leading substrate with respect to ubiquitin in both steps 1 and 3, and the PP_i formed in step 1 the leading product with respect to AMP (Haas & Rose, 1982).

In the absence of ATP, isopeptide bond formation may proceed from the enzyme–ubiquitin thiol ester complex in steps catalyzed by additional enzymes of the system (Haas et al., 1982). Since the carboxyl-terminal glycine of ubiquitin is involved in the thiol ester linkage to the enzyme (Hershko et al., 1981), the ubiquitin adenylate has been assumed to exist as a mixed acyl phosphate anhydride between the carboxyl

† From the Institute for Cancer Research, Fox Chase Cancer Center, Philadelphia, Pennsylvania 19111. *Received April 11, 1983.* This work was supported by National Institutes of Health Grant GM-20940 and American Cancer Society Grant BC-414 to I.A.R. and National Institutes of Health Grants CA-06927 and RR-05539 and an appropriation from the Commonwealth of Pennsylvania to the Institute for Cancer Research.

‡ Present address: Department of Biochemistry, The Medical College of Wisconsin, Milwaukee, WI 53226.

[1] Abbreviations: Ub, ubiquitin; AMP–Ub, ubiquitin adenylate; BSA, bovine serum albumin; HPLC, high-performance liquid chromatography; etheno-ATP, 1,N^6-ethenoadenosine 5′-triphosphate; etheno-CTP, 3,N^4-ethenocytidine 5′-triphosphate; ATPαS, adenosine 5′-*O*-(1-thiotriphosphate); ATPβS, adenosine 5′-*O*-(2-thiotriphosphate); ATPγS, adenosine 5′-*O*-(3-thiotriphosphate); $ADPCH_2P$, adenosine 5′-(β,γ-methylenetriphosphate); ADPNHP, 5′-adenylyl imidodiphosphate; Na$DodSO_4$, sodium dodecyl sulfate; DTT, dithiothreitol; TPCK, L-1-(tosylamido)-2-phenylethyl chloromethyl ketone; Tris, tris(hydroxymethyl)aminomethane; EDTA, ethylenediaminetetraacetic acid; NTP, nucleoside triphosphate; Cl_3CCOOH, trichloroacetic acid.

0006-2960/83/0422-4388$01.50/0